Final Report for AOARD Grant 104048

"**Metal Nanoshells for Enhanced Solar-to-Fuel Photocatalytic Conversion**"

Date 09/20/2011

Name of Principal Investigators: Tai-Chou Lee

- e-mail address : taichoulee@ncu.edu.tw
- Institution : Department of Chemical Engineering, National Chung Cheng University
- Mailing Address : 168 University Road, Min-Hsiung, Chia-Yi 621, Taiwan
- Phone : +886-3-4227151-34211
- Fax : +886-3-4252296

Period of Performance: 03/07/2010 – 09/07/2011

Abstract

In our preliminary study, we had prepared quaternary semiconductor powder of $Ag_xIn_xZn_yS_{2x+y}$, a photocatalysts with a high activity. In this study, we further extended the investigation, changed the amount of indium in a series of solid solutions, and increased the photochemical activity substantially. With little adjustment of the ratios of [In]/[Ag], the hydrogen production rate of the photocatalysts, $Ag_xIn_yZn_zS_{(x+3y+2z)/2}$, are significantly improved. The most enhancement of the activity can go up to four times, compared to our first generation photocatalyst. SEM images show that different amount of nonosteps on the surface relate to the ratios of [In]/[Ag]. These edges of nanosteps are considered as the active sites that facilitate the electron-hole separation, leading to higher solar-to-fuel conversion efficiency. The other ingredient, zinc, is used to control the band gap. Both changes of indium and zinc, we maximized the efficiency of this photocatalyst (970 μmol/h·g). In a separate experiment, the photocatalystic reactions were carried out at elevated temperature. The effect of temperature, typically with addition of Ag@Au NPs (nanoparticles) was evaluated. The presence of metal nanoshells can absorb the solar energy in the IR range. However, the broad absorption of metal nanoshells also covered the visible-light region, which decrease the efficiency of the metal sulfide photocatalysts. The incorporation of metal nanoshells, as well as the nanostructure of photocatalyst will be further investigated.

Introduction

Of all known renewable energy sources, solar energy stands as the most abundant and readily accessible. Consider, for example, that the amount of solar energy striking the earth every 40 minutes

Report Documentation Page

Form Approved
OMB No. 0704-0188

1. REPORT DATE	2. REPORT TYPE	3. DATES COVERED
22 SEP 2011	**Final**	**03-09-2010 to 09-09-2011**

4. TITLE AND SUBTITLE	5a. CONTRACT NUMBER
Metal Nanoshells for Enhanced Solar-to-Fuel Photocatalytic Conversion	**FA23861014048**
	5b. GRANT NUMBER
	5c. PROGRAM ELEMENT NUMBER
6. AUTHOR(S) **Tai-Chou Lee**	5d. PROJECT NUMBER
	5e. TASK NUMBER
	5f. WORK UNIT NUMBER
7. PERFORMING ORGANIZATION NAME(S) AND ADDRESS(ES) **National Central University,No.300, ,Jhongda Rd,Jhongli City TaoyuanTaiwan,TW,320**	8. PERFORMING ORGANIZATION REPORT NUMBER **N/A**
9. SPONSORING/MONITORING AGENCY NAME(S) AND ADDRESS(ES) **AOARD, UNIT 45002, APO, AP, 96338-5002**	10. SPONSOR/MONITOR'S ACRONYM(S) **AOARD**
	11. SPONSOR/MONITOR'S REPORT NUMBER(S) **AOARD-104048**

12. DISTRIBUTION/AVAILABILITY STATEMENT
Approved for public release; distribution unlimited

13. SUPPLEMENTARY NOTES

14. ABSTRACT

Preparation of next-generation photocatalysts is presented. The indium content in this four-component photocatalyst was found to play a critical role. The highest hydrogen evolution rate is 970 μmol/h?g. The [Zn]/[Ag] also determined the utilization of visible-light region in the solar spectrum. Samples with various [Zn]/[Ag] compositions show different photocatalytic activities in full spectrum and in visible light. Secondly, it was demonstrated that at an elevated temperature, the hydrogen evolution rate is higher. Future study will focus on improving the efficiency of our second-generation photocatalyst, create various core-shell structures, measure the hydrogen production rate, and test the stability of this composite system.

15. SUBJECT TERMS
Metal Nanoshells, Metal Nanoshells, Photocatalysts, Hydrogen Generation

16. SECURITY CLASSIFICATION OF:			17. LIMITATION OF ABSTRACT	18. NUMBER OF PAGES	19a. NAME OF RESPONSIBLE PERSON
a. REPORT **unclassified**	b. ABSTRACT **unclassified**	c. THIS PAGE **unclassified**	**Same as Report (SAR)**	**11**	

is approximately equal to the amount of energy consumed globally on an annual basis.[1] From this perspective, the United States is fortunate to have vast tracts of land that are suitable for constructing solar power plants; in fact, in the desert Southwest alone there are an estimated 250,000 square miles of suitable land receiving more than 4,500 quadrillion British thermal units (Btu) of solar radiation per year.[1] Converting only 2.5% of that radiation into electricity would equal the total national energy consumption during all of 2006.[1]

The abundance and availability of solar energy has sparked the exploration of a wide variety of solar conversion technologies, including those based on photovoltaics (direct solar to electric), photothermal (solar to heat), and photosynthesis (solar to fuel). In the latter technology, artificial photosynthesis mimics natural photosynthesis by converting water and/or carbon dioxide into fuels and oxygen using sunlight. Splitting water to produce hydrogen and oxygen is one example, and it is the most promising replacement for fossil fuels without any pollutant[2-4]. The development of visible-light-driven photocatalysts for water splitting is critical. ZnS is a highly active photocatalyst for H_2 evolution under UV light irradiation[5-6]. Because of its wide band gap, the conduction band level is high enough to reduce water. $(AgIn)_xZn_yS_{2x+y}$ solid solution, derived from ZnS is a narrower band gap semiconductor. The absorption of the solid solutions can be tuned from UV light to visible light by adjusting $ZnS/AgInS_2$ ratio. $AgInZn_7S_9$ with a high efficiency of H_2 production is a typical example (~3.3 L/m^2-h).[7] $AgInZn_7S_9$ solid solution with 2.35 eV band gap absorbs the wavelength below 600 nm[8]. For wavelength longer than 600 nm, the light cannot be utilized effectively. This fact has motivated us to search for materials or composite materials that can utilize as much solar energy as possible.

Metal-metal nanoshells (Ag@Au) can absorb the light at different wavelength[9] by altering the thickness of nanoshell (Au). The nanoparticles have an absorption edge in the IR range (>700 nm) can convert the solar energy to heat. According to reaction kinetics, the water splitting reaction rate increases with the temperature. In this study, we wish to explore the development of a unique solar-to-fuel conversion system that is based on recent advances in nanotechnology. In the first part of the report, our second-generation photocatalyst was investigated. The composition ratios of Ag/In and Ag/Zn are two key factors for photocatalytic activity. Secondly, we reported the H_2 evolution rate of $AgInZn_7S_9$ solid solution at elevated temperatures and then compared to the results with the addition of nanoparticles (NPs) to see the effect of temperature enhancement by Ag@Au NPs.

Experiment

1. *Preparation of photocatalyst*

An aqueous solution of $AgNO_3$ (J.T. Baker; 100 %), $In(NO_3)_3 \cdot xH_2O$ (Alfa Aesar; 99.99 %), $Zn(NO_3)_2 \cdot 6H_2O$ (J.T. Baker; 100 %), and NH_4NO_3 (Riedel-de Haen; 98 %) was prepared in a 100 mL round bottomed flask and mixed well. The pH value of the solution was then adjusted to be around 1 by adding concentrated H_2SO_4. Thioacetamide (TAA, Sigma Aldrich; 99 %) was used as the S^{2-} source.

Prescribed molar ratios in the precursor solutions are listed in Table 1. After 5 h of reaction, the precipitates were rinsed thoroughly with deionized (DI) water several times, and they were then dried at 80 °C in an oven for 12 h. The obtained powders were heat treated at 800 °C for 1 h in an ultrapure N_2 environment in a tube furnace. A Pt co-catalyst was loaded by the photodeposition method in situ by using $H_2PtCl_6 \cdot {}_6H_2O$ (Uniregion Bio-tech; 99.95 %).

Table 1. Compositions of the precursor solutions.

Sample	Ag	In	Zn	TAA
A	1	1	7	10.5
B	1	1.25	7	10.5
C	1	1.5	7	10.5
D	1	1.75	7	10.5
E	1	2	7	13.5
F	1	1.75	3	13.5
G	1	1.75	4	13.5
H	1	1.75	5.5	13.5
I	1	1.75	8.5	13.5
J	1	1.75	10	13.5

Co-catalyst (Pt) was loaded on particle surface by photodeposition. Pt (3 wt%) was loaded by photodeposition in N_2 gas at a pressure of 40 torr and 20 °C from the solution of $H_2PtCl_6 \cdot 6H_2O$ dissolved in methanol. The co-catalyst-loaded photocatalysts were collected by filtration, washed with water, and then dried at room temperature in air.[10] The oxidation states of the metal-loaded photocatalysts were investigated by using XPS. Fig. 1 illustrates the Pt 4 f doublet. The binding energy of 72.678 eV is reduction state of metal Pt. The peak at 73.850 eV has a higher binding energy, which is attributed to the un-reacted H_2PtCl_6.

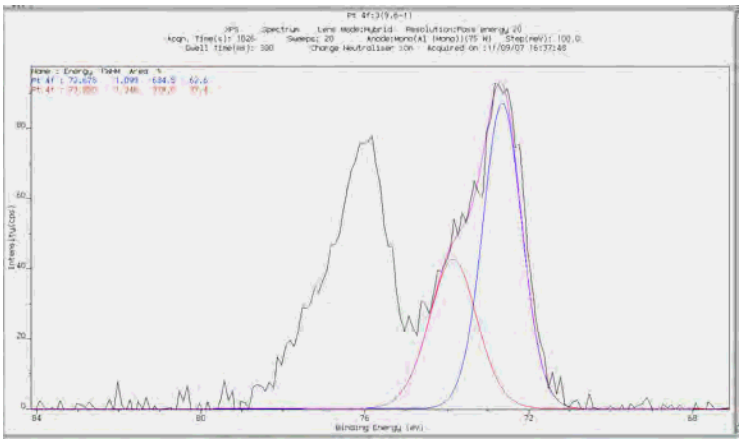

Fig. 1. XPS spectrum of 3 wt% Pt-loaded $AgInZn_7S_9$.

2. *Photochemical Reaction*

Photocatalytic reactions were conducted in a home-made glass cell with a quartz side window. The 300 W Xenon lamp was employed to simulated the sun light whose light path was adjusted and focused on a uniform illumination at the quartz window (Fig. 2). The photocatalyst powders, loaded with Pt (3 wt%) were dispersed in an aqueous solution containing sacrificial reagents (220 mL of 0.25 M K_2SO_3 and 0.35 M Na_2S) with magnetic stirring. They were then reacted under a Xe lamp. Hydrogen gas was collected by using the water displacement method under 100mW/cm^2 irradiation, with and without UV-cut filter (> 400 nm).

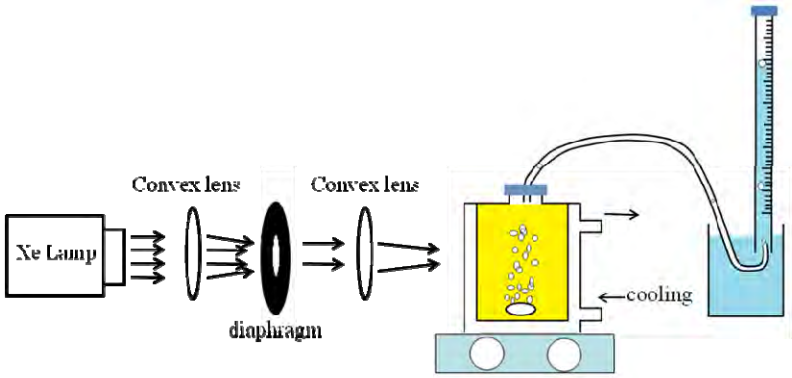

Fig. 2. Photocatalytic reaction system.

3. *Preparation of Silver nanoparticles (NPs)*

Silver NPs were prepared by using the slightly modified Lee and Meisel method[11]. A solution of 1 mM $AgNO_3$ (100 mL) in a 250 mL flask was heated, and 2 mL of 1 % sodium citrate (Sigma Aldrich) solution was added as soon as the $AgNO_3$ solution began boiling[9]. The yellowish solution turned to greenish after the addition trisodium citrate. After 45 min of reaction, the Ag NPs were collected by centrifuge for 20 min at 4000 rpm (3 times), and then filtered through 0.22 μm membrane filter to remove the Ag nanorods. The SEM image (Fig. 3) shows that the size of Ag NP is 60 ~ 80 nm.

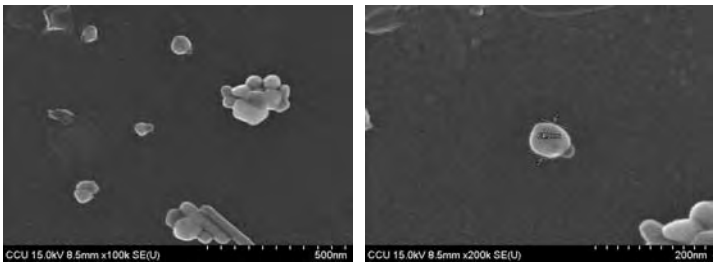

Fig. 3. SEM images of Ag NPs. The size is around 60~80 nm.

4. *Gold nanoshell growth*

K-Gold solution was prepared by dissolving 0.025 g of K_2CO_3 (J.T. Baker; 99.8 %) in a mixture of

water (100 mL)[12-13]. After stirring for 10 min, an aliquot (1 %, 2 mL) of $HAuCl_4$ solution was added. The solution changed from yellow to colorless in 30 min, and then kept in dark overnight. An aliquot (8 mL) of K-Gold solution was placed in a 20 mL qorpak containing a magnetic stirring bar, and then varying amounts of silver NPs were added to produce gold shells of various thicknesses.

Results and Discussion

In published papers,[7, 14] the amount of zinc sulfide was considered the major parameter to adjust the band gap energy of $Ag_xIn_xZn_yS_{2x+y}$. The position of conduction band relates to the efficiency of hydrogen production and is determined by the band gap energy. In the first section, we found that one additional parameter [In]/[Ag] play a critical role in hydrogen production. An increase in hydrogen evolution rate was observed for various [In]/[Ag] ratios, when [Zn]/[Ag] = 7 was kept constant (Fig. 4). In this experiment, we essentially maintain the band gap energy as a constant and controlled the solar-to-fuel efficiency by tuning the amount of indium sulfide. The composition of the photocatalyst can be referred to Table 1.

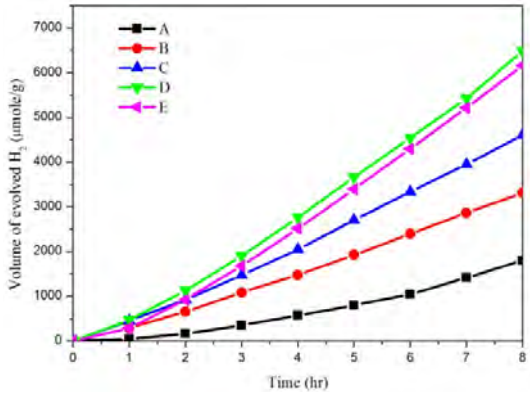

Fig. 4. Hydrogen evolution for samples with various ratio of [In]/[Ag].

The sample B ([In]/[Ag] = 1.25) is the most remarkable example to show that the activities was enhanced by increasing the ratio of [In]/[Ag] (see Fig. 4). 25% more indium doubled the evolution rate of hydrogen. This trend is maintained until Sample D ([In]/[Ag] = 1.75), which is the parameter to produce the highest hydrogen evolution rate, 930 μmol/h·g.

The solid solutions of $Ag_xIn_xZn_yS_{2x+y}$ have specific nanostep structures.[7] The edges on the photocatalysts surface are believed to be the reduction sites for photocatalytic reactions.[7] Fig. 5 shows the SEM images of these photocatalysts. It can be observed that relatively more nanostep structures appeared on the samples with higher [In]/[Ag] ratio. Sample D has the most nanosteps, which consists with the hydrogen production rate shown in Fig. 4. These results suggested that perhaps the content of indium is one of the major factors to create nanosteps on the surface of the catalyst. The photocatalytic activity is proportional to the amount of active sites.

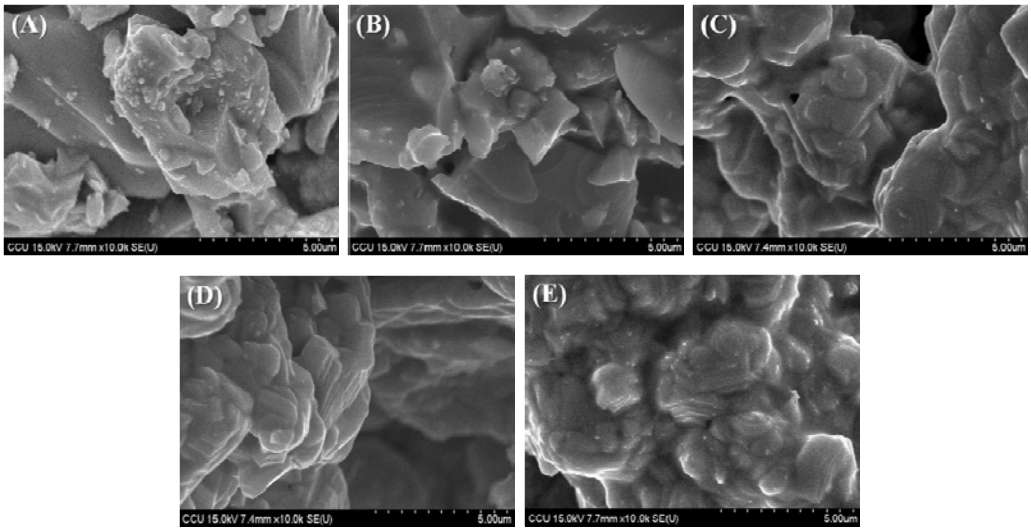

Fig. 5. SEM images of samples with various ratio of [In]/[Ag].

The phase diagram of AgS_2 - In_2S_3 shows that the single phase of $AgInS_2$ has a small operating window.[15] Equal molar of AgS_2 and In_2S_3 is required for the formation of the single phase $AgInS_2$. The excess or deficit of indium will cause the formation of $AgInS_2$-$AgIn_5S_8$ or Ag_2S-$AgInS_2$ coexistence phase, respectively. However, no phase diagrams have been reported in the literature, regarding different ratio of [In]/[Ag] in the ZnS – Ag_2S- In_2S_3 system. Fig. 6 shows that the XRD diagram of five samples. All of them have similar structures, corresponding to the solid solution of ZnS-$AgInS_2$ with a hexagonal structure, except a shift observed at higher diffraction angles. The ion radius of indium is larger than the other two ions (silver and zinc). It is expected that peaks shift to lower angles as [In]/[Ag] ratio increases from 1 (sample A) to 2 (sample E).

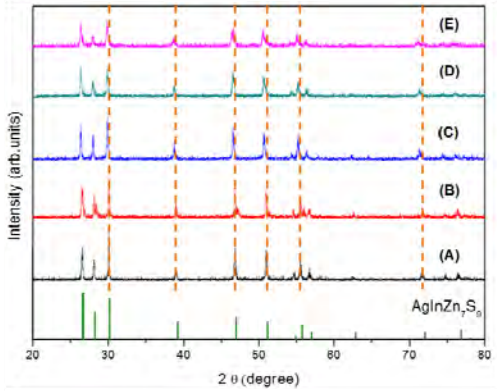

Fig. 6. Powder XRD patterns for samples with various ratio of [In]/[Ag].

In the second section, we changed band gap energies by tuning the ratio of [Zn]/[Ag] and kept the ratio of [In]/[Ag] at 1.75. UV light provides high energy photon to split water, but also oxides S^{2-} to S and causes the photocorrosion. However, illuminated by light with UV-cut filter also reduce the hydrogen production rate. By tuning the [Zn]/[Ag] ratio, the optimal band gap energy in visible-light

region can be determined.

Without UV-cut filter, Sample I ([Zn]/[Ag] = 8.5) has the highest photocatalytic activity (970 μmol/h·g). However, Sample H ([Zn]/[Ag] = 5.5) has the highest photocatalytic activity after filtering out UV light (Fig. 7). A higher [Zn]/[Ag] ratio leads to a higher band gap energy solid solution. In theory, a smaller band gap semiconductor can utilize more energy from the sun light. Our experimental results indicate that the utilization of solar spectrum depends on many factors, giving rise to an optimal composition. As shown in Fig. 8, we compared the difference between illumination with and without UV-cut filter for each photocatalyst. The red-shift in absorption spectra (Fig. 9) follows the decrease in [Zn]/[Ag] ratio. This ratio which exhibits largest difference between with and without UV-cut filter is 8.5. Here, UV light provides approximately 45% of energy to split water. As the [Zn]/[Ag] ratio decreases, the decay of evolution rate become smaller with UV-cut filter. The longer wavelength light dominates the photoreaction in smaller [Zn]/[Ag] samples.

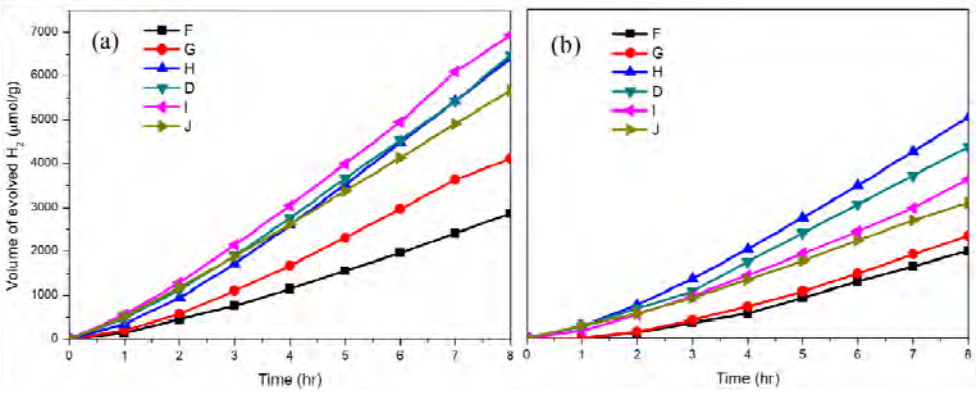

Fig. 7. Volume of evolution for (a) without UV filter; (b) UV filter.

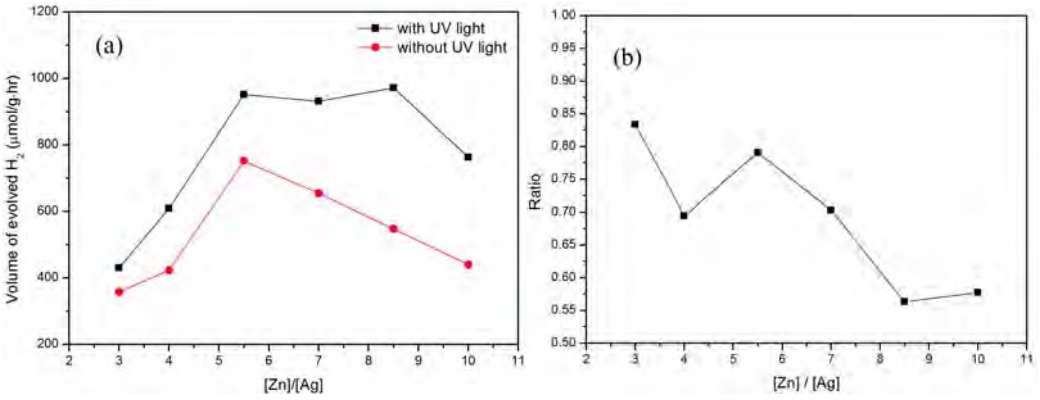

Fig. 8. (a) Photocatalytic H_2 evolution under Xe lamp with UV light and without UV light, (b) evolution ratio of (visible light)/(UV and visible light) as a function of [Zn]/[Ag].

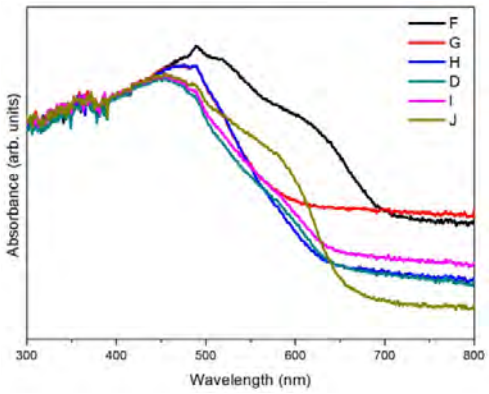

Fig. 9. The UV-Vis absorption patterns for samples with various amount of Zinc.

We further measure the absorption of photocatalyst using UV-Vis spectrometer (Fig. 9). Sample F ([Zn]/[Ag] = 3.0) absorbs the longest wavelength (> 600 nm). However, the photovoltage is too low to drive the water splitting reaction. The absorption of Sample H, D and I are quite similar, but Sample H absorbed higher intensity of green light (500 nm, 2.48 eV) than the other two samples. A slightly blue-shift in absorption edge was observed as [Zn]/[Ag] ratio increases. Fig. 10 is the XRD patterns of the samples with various [Zn]/[Ag] ratios, from 3 (sample F) to 10 (sample J). A shift in the XRD peak positions to a higher angle was observed, which agrees with those found in the literature[8].

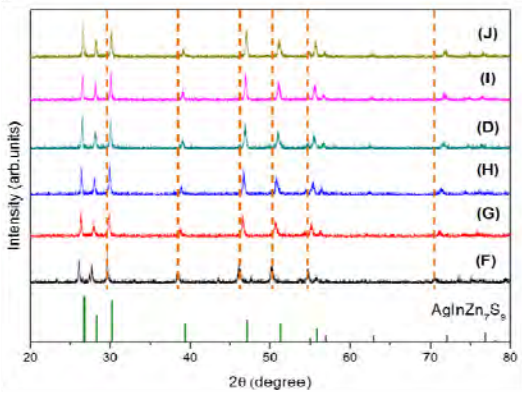

Fig. 10. Powder XRD patterns for samples with various ratio of [Zn]/[Ag].

In the second part of the report, we first compared the hydrogen evolution rate at two reaction temperatures (Fig. 11). It can be seen that the efficiency at 80 °C is higher than that carried out at 20 °C. This proof of concept experiment has demonstrated that temperature effect can facilitate the water splitting. The steady hydrogen evolution rate increases by 500 %.

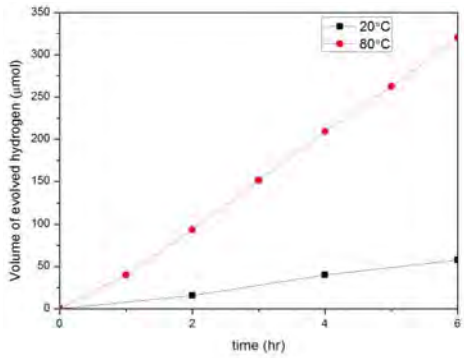

Fig. 11. The efficiency of hydrogen evolution at 80 °C and 20 °C.

We measured the hydrogen production rate of $AgInZn_7S_9$ with silver NPs and compare to that without NPs. Fig. 12 shows that the efficiency of photcatalysts with Ag NPs is lower than bare photocatalysts at longer time. This background experiment is to show that because Ag NPs absorbed the light in the region overlap with photocatalysts, it hinders the hydrogen production rate. We have to choose suitable NPs in order to increase the reaction temperature and/or improve the stability of the photocatalysts.

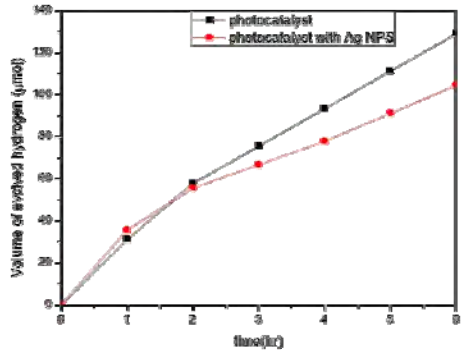

Fig. 12. Hydrogen production-effect of Ag NPs.

The metal-metal NPs (Ag@Au) can adjust absorption at different wavelength by changing the relative volume of Ag NPs and K-gold solution[9], listed in Table 2. The prepared nanoparticles can absorb infrared light. We first need to verify that the presence of NPs can increase the solution temperature upon irradiation. These NPs were added to the solution, and the variation of the temperature of the reaction cell were recorded under a 300 W Xe lamp illumination. Fig. 13 shows the nanoshells indeed increase the solution temperature upon irradiation. Our next strategy to incorporate metal nanoshells into our photocatalytic system is 1: synthesize uniform distributed metal nanoshells, and 2. Create an inverse structure, i.e. metal-nanoshell core/photocatalysts shell structure. Solar energy in the visible-light range is expected to be absorbed by the photocatalyst first without any interference of the metal nanoshells. These topics are under investigations.

Table 2. Composition and absorption of core-shell (Ag@Au).

sample	volume ratio		Absorption (nm)
	Ag NPs	K-Gold solution	
A	1	8	810
B	2	8	730
C	3	8	800
D	4	8	670
E	5	8	650

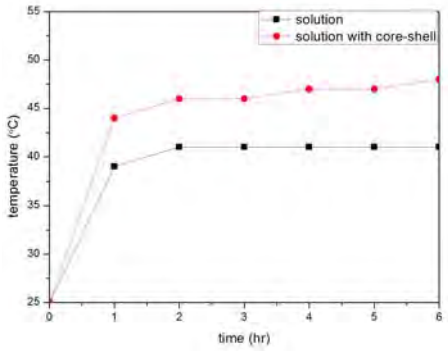

Fig. 13. Temperature effect of core-shell (Ag@Au).

In summary, we first reported the preparation of our next generation photocatalysts. The indium content in this four component photocatalyst was found to play a critical role. The highest hydrogen evolution rate is 970 μmol/h·g. The [Zn]/[Ag] also determined the utilization of visible-light region in the solar spectrum. Samples with various [Zn]/[Ag] compositions show different photocatalytic activities in full spectrum and in visible light. Secondly, we demonstrated that at an elevated temperature, the hydrogen evolution rate is higher. In the future study, we will improve the efficiency of our second-generation photocatalyst, create various core-shell structures, measure the hydrogen production rate, and test the stability of this composite system.

Reference

1. Zweibel, K.; Mason, J.; Fthenakis, V., *Sci. Am.* **2008**, Jan., 64-73.
2. Kudo, A., *Int J Hydrogen Energ* **2007,** *32*, 2673-2678.
3. Kudo, A.; Sekizawa, M., *Chemical Communications* **2000**, 1371-1372.
4. Chen, D.; Ye, J., *Journal of Physics and Chemistry of Solids* **2007,** *68*, 2317-2320.
5. Reber, J.-F.; Meier, K., *Journal of Physical Chemistry* **1984,** *88*, 5903-5913.
6. Zeug, N.; Bucheler, J.; Kisch, H., *J Am Chem Soc* **1985,** *107*, 1459-1465.
7. Tsuji, I.; Kato, H.; Kobayashi, H.; Kudo, A., *J. Am. Chem. Soc.* **2004,** *126*, 13406-13413.

8. Tsuji, I.; Kato, H.; Kobayashi, H.; Kudo, A., *J Am Chem Soc* **2004,** *126*, 13406-13413.

9. Yang, Y.; Shi, J. L.; Kawamura, G.; Nogami, M., *Scripta Mater* **2008,** *58*, 862-865.

10. Sasaki, Y.; Nemoto, H.; Saito, K.; Kudo, A., *The Journal of Physical Chemistry C* **2009,** *113*, 17536-17542.

11. Lee, P. C.; Meisel, D., *The Journal of Physical Chemistty* **1982,** *86*, 3391-3395.

12. Ji, X. J.; Shao, R. P.; Elliott, A. M.; Stafford, R. J.; Esparza-Coss, E.; Bankson, J. A.; Liang, G.; Luo, Z. P.; Park, K.; Markert, J. T.; Li, C., *J Phys Chem C* **2007,** *111*, 6245-6251.

13. Phonthammachai, N.; Kah, J. C. Y.; Jun, G.; Sheppard, C. J. R.; Olivo, M. C.; Mhaisalkar, S. G.; White, T. J., *Langmuir* **2008,** *24*, 5109-5112.

14. Kudo, A.; Tsuji, v.; Kato, H., *Chem. Commun.* **2002**, 1958-1959.

15. Sachanyuk, V. P.; Gorgut, G. P.; Atuchin, V. V.; Olekseyuk, I. D.; Parasyuk, O. V., *J. Alloy. Compd.* **2008,** *452*, 348-358.

List of Publications

Conference presentations

1. P.-C. Lin and T.-C. Lee, “Prepare $(AgIn)_xZn_{2(1-x)}S_2$ Solid-Solution Film for Photoelectrochemical Water Splitting”, International Conference on Materials for Advanced Technologies ICMAT 2011, 6/26-7/1/2011, Singapore.

2. T.-C. Lee, “Photocatalytic Properties of Metal Sulfide Thin Films and Powders”, 14^{th} Asian Chemical Congress 2011, 9/5-9/8/2011, Bangkok, Thailand.